

Optimized Control of an Electric Vehicle With Functional Actuator Redundancy

Peter Bergmiller, Fabian Schuldt, Markus Maurer
Technische Universität Braunschweig
38106 Braunschweig, Germany
Email: {bergmiller, schuldt, maurer}@ifr.ing.tu-bs.de

Abstract—This paper proposes an approach for optimized control of vehicle actuators as far as wear of individual components is concerned. The system is intended to improve the performance of existing balancing and protection systems working on component level. Well-tested and commonly known optimization algorithms are integrated into the onboard software to handle mutual dependencies of wear of components by generating an optimal coordination strategy. A suitable system architecture facilitates safe operation of the system and reduction of computational load. The approach especially focuses on electric vehicles with functional actuator redundancy and several power-supply units.

Proper operation of the algorithm is demonstrated based on a full electric experimental vehicle. Thereby, tire wear is balanced while equalizing usage of the traction batteries and temperature levels of the drive motors.

I. INTRODUCTION

Modern automobiles feature a multitude of actuators and power consuming units. Thus, proper coordination of the actuators is important to optimize energy efficiency and to avoid overload of individual components. This increases the lifetime of the vehicle and contributes to driver safety, as critical components of the drive train are protected. In full electric vehicles (EVs) the situation becomes even more challenging. The total available energy for driving is strongly limited and expensive components of the drive train (e. g., batteries or inverters) have to be protected from overloads. At the same time, EVs can provide additional degrees of freedom for vehicle control, e. g., the option to drive individual wheels or to recuperate braking energy [1], [2].

This paper proposes an approach for optimal coordination of actuators in an EV to achieve balanced load, and thus wear, for components of the drive train (Fig. 1). Additionally, reduction of overall wear seems possible, but is not main focus of this paper. A flexible experimental vehicle featuring four-wheel drive, one motor per axle, four wheel steering and one power supply per axle serves as test bed (Fig. 2).

Related Work and Contribution of This Paper

Reduction and balancing of wear as well as protection of expensive components is already an important goal in the design of modern vehicles. According measures target at the mechanical design as well as vehicle electronics:

- A proper design of the steering geometry reduces tire wear while driving curves, e. g., the ackermann-steering geometry is proposed for driving at low speed [3].

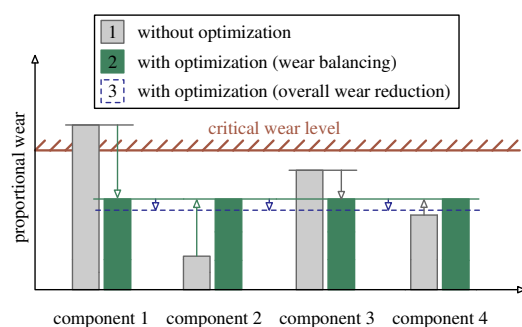


Fig. 1. Balancing of wear of multiple components and overall wear reduction

- Battery Management Systems ensure safe operation of the drive battery in EVs or Hybrid-EVs [4], [5].
- Energy Management units in series vehicles prioritize power consuming units and control energy distribution in the onboard network [6].
- Start-Stop Systems switch off combustion engines during short halts of the vehicle to save fuel if sufficient electrical energy is available for a quick restart [7].

In operations research, similar challenges have to be solved. Thereby, the output of an industrial plant has to be increased while dealing with restricted resources. E. g., Alcaraz et al. and Zhang et al. discuss different genetic algorithms to minimize lead times in production processes with mutual dependencies, parallel actions and several constraints [8], [9].

The proposed approach combines existing research results to add a coordination layer on overall vehicle level for further improvement of energy and load management. Mutual dependencies of system components are taken into account

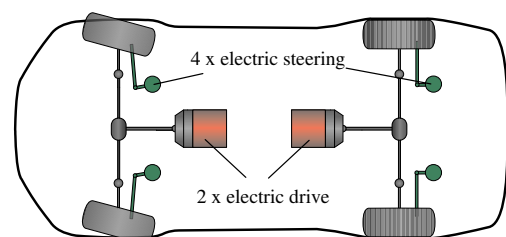


Fig. 2. Schematic overview of the experimental vehicle

and new actuator flexibilities provided by EVs are exploited. For demonstration, a simplified, but highly real-time critical scenario dealing with tire wear is chosen.

II. SYSTEM ARCHITECTURE

The system architecture plays a key role to safely integrate optimization algorithms into a safety-critical real-time system. Therefore, the following requirements were defined:

- Safe operation of the vehicle has to be guaranteed also in case of failure of the optimization system.
- The optimizer must not modify lateral vehicle handling. Longitudinal handling can be influenced in case vital components, e. g., the batteries, have to be protected.
- Requirements on computational power should be adjustable depending on the demanded quality of results.

A. Integration of the Optimization Algorithm

Fig. 3 shows the system architecture proposed by this work. Driver commands are transmitted to a drive controller. The drive controller derives commands for the actuators. Thereby, the controller can perform simple command forwarding or emulate desired vehicle behavior. The commands by the drive controller are passed to the distribution unit. There, the optimizer modifies the commands to balance wear and prevent overload of individual components. The modified commands are forwarded to the actuators. The optimizer is fed with the driver commands, constraints for the optimization tasks and the current vehicle state. This architecture provides several advantages that allow to fulfill the requirements given above:

1) *Execution Frequency*: The execution frequency of the optimizer is adjustable independently from the execution time of the real-time control task. If the optimizer does not update the distribution pattern in the distribution unit, the previous distribution pattern is kept until an update is received. This is especially useful if the optimization goals change slowly compared to the driver inputs or vehicle dynamics. Then, the update rate can be lowered, and thus computational load is reduced.

2) *Driver Perception*: Driver perception of interventions by the optimizer is limited, as constraints prohibit interventions of the optimizer that influence vehicle handling

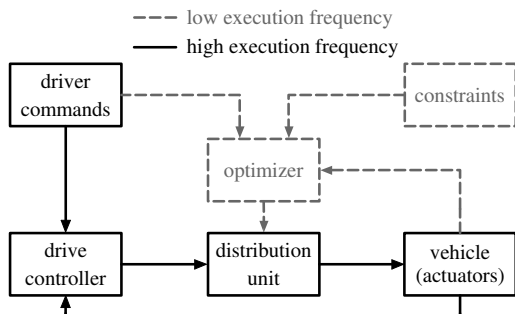


Fig. 3. System architecture with optimization functionality

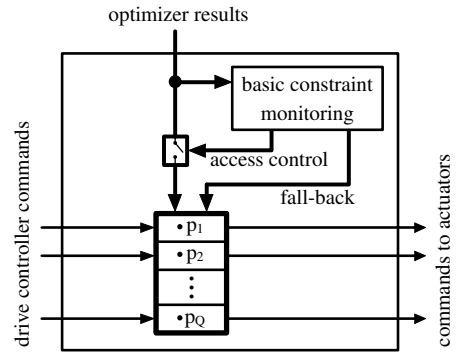


Fig. 4. Internal structure of the distribution unit

significantly. Additionally, the drive controller compensates remaining influences. Experiments have shown that these measures ensure adequate vehicle handling.

3) *Safety*: As detailed in the following section, the distribution unit serves as monitoring and safety system. It can easily decouple the optimizer from the main signal path for vehicle control in case of errors.

B. Fault Compensation

Fig. 4 details the internal structure of the distribution unit. During normal operation, the optimizer sets the distribution parameters p_1 to p_Q according to the calculated optimal solution. The command values from the drive controller are multiplied with these parameters. A monitoring subsystem checks the commanded parameters for compliance with basic constraints. A basic constraint can, e. g., be that the average of the left and the right steering angle has to equal the steering angle commanded by the driver. If a failure occurs or critical driving maneuvers are detected, the distribution unit separates the optimizer from the signal path. Thus, a safe fall-back operation can be achieved. In case of transient failures, the old distribution parameters are kept and the faulty update is discarded. If long-term malfunctions are detected, the parameters are reset to save default values.

III. SELECTION OF AN OPTIMIZATION ALGORITHM

The automotive application puts special demands on the used optimization algorithm. For this work, different approaches were evaluated based on the following criteria:

- Low requirements on computational power facilitate frequent updates of results and usage of cheaper hardware.
- If possible, the solution generated by the optimization algorithm should be a global optimum.
- Good usability of the algorithm is desirable to facilitate usage in different application scenarios.

As a result of the evaluation, an approach for multi object optimization (MOO) was chosen. This allows the developer to easily integrate new optimization goals into the system. To solve the MOO problem, evolutionary and gradient based optimization approaches were compared. Evolutionary optimization algorithms are less susceptible to local minima,

while gradient based systems feature significantly lower execution times. Due to the execution times, a gradient based algorithm was chosen and combined with a multi-start strategy to improve the performance to detect a globally optimal solution. The optimization problem was solved by the sequential quadratic programming algorithm (SQP) [11] due to its superior computational performance [12]. For comparisons with evolutionary systems, the Multi Objective Model Based Evolution Strategy (MOMBES) introduced by Meyer was used [10].

IV. OPTIMIZATION CRITERIA AND CONSTRAINTS

To balance wear of components, optimization criteria and constraints focusing on tire wear, temperature of actuators and state of charge (SOC) of the power supplies in the experimental vehicle are defined. Thereby, wear is not only balanced between units of the same type, but also across different types, e. g., between motors and tires. Additionally, temporary overload and in-total critical wear are taken into account. To achieve these goals, relative and absolute measures are introduced to quantify the wear of a component.

A. Constraints

Constraints ensure that the interventions of the optimizer during normal operation of the vehicle are not noticeable by the driver, and actuator limitations are obeyed. The proposed application includes the following constraints:

- *Actuator limits:* For temperatures, torques and steering angles maximal/minimal values are set.
- *Maximal change:* The maximal acceptable change per time step of each of the distribution parameters p_1 to p_Q is limited to avoid rapid changes in vehicle handling.
- *Command forwarding:* The mean value of left and right steering angle commanded by the optimizer has to equal the reference set by the driver. As long as a linear tire model approximates reality, this makes interventions of the optimizer imperceptible by the driver. In highly dynamic driving scenarios, the optimizer is turned off.

B. Optimization Criteria

Based on optimization criteria, the optimizer evaluates the current situation and short term predicts the effects of a set of commands on objective attainment. This section introduces a set of criteria implemented to achieve balanced wear and overload protection for components.

1) *Reference Torque:* Deviation of the torque command sent to the motors from the reference torque set by the driver is minimized. Thus, the mean value of all torque commands in the experimental vehicle should equal the torque reference set by the driver. Deviations are only acceptable if expensive components as the motors or the battery have to be protected from, e. g., over-heating. The corresponding normalized optimization criterion $n_M(t)$ for the current point in time t is calculated according to:

$$n_M(t) = \frac{G \cdot M_{set}(t) - \sum_{g=1}^{g=G} M_g(t)}{M_{set}(t)}, \quad (1)$$

where $M_g(t)$ denotes the commanded torque for motor g , G the total number of motors and $M_{set}(t)$ the torque per motor demanded by the driver. The normalization is required to guarantee the same scale for all optimized inputs before weighting the criteria relative to each other.

2) *Tire Wear:* The optimization criterion "tire wear" focuses on a common problem especially in metropolitan areas where one tire of an axle or both tires of one axle are used up more than other tires. The driver has to perform maintenance on the car as soon as one of the tires can no longer guarantee safe driving or features a tread depth below the one required by law. The optimizer tries to balance the tire wear. According to Huang et al. [13], one of the main influence factors on tire wear is the tire slip. Therefore, a simplified online estimation of tire wear in the experimental vehicle is implemented based on tire slip and was verified in practical experiments:

- 1) The normal forces F_{N_i} are calculated for each of the $i = 1..4$ wheels based on static weight distribution and dynamic loading of each wheel.
- 2) The longitudinal slip s_{l_i} of each tire is estimated. As the slip estimation is not focus of this paper, the following empirical formula identified based on simulation results and real measurements is implemented:

$$s_{l_i} = (0.8 \cdot |\delta_i| + 1) \cdot (0.007 \cdot (M_i - 0.0453 \cdot v_i^2)). \quad (2)$$

δ_i denotes the steering angle in radians, M_i the torque in Nm and v_i the speed at wheel i in $\frac{m}{s}$.

- 3) The lateral slip s_{s_i} is estimated according to [14]. For a driven wheel the absolute value is calculated as:

$$s_{s_i} = |\tan(\alpha_i)|. \quad (3)$$

α denotes the side slip angle of the current tire determined based on the current speed, side slip angle of the vehicle and yaw rate.

- 4) The overall tire slip s_i is calculated according to [14]:

$$s_i = \sqrt{s_{l_i}^2 + s_{s_i}^2}. \quad (4)$$

- 5) As the optimizer is only supposed to operate during normal driving, a linearized function to calculate the current friction coefficient is used:

$$\mu_{eff_i} = C \cdot s_i \quad (5)$$

The proportional factor C was determined based on practical experiments with the experimental vehicle.

- 6) Based on μ_{eff_i} , the vehicle speed at wheel i and the normal forces F_{N_i} , the power P_i transmitted by each wheel is approximated as:

$$P_i = \mu_{eff_i} \cdot F_{N_i} \cdot v_i. \quad (6)$$

- 7) The transmitted power of the i -th wheel is integrated over time to determine the transmitted energy $W_i(t)$ up to the current point in time t . $W_i(t)$ is used to approximate the tire wear of the i -th wheel.

8) The resulting $W_i(t)$ are normalized each time step:

$$n_{W_i}(t) = 0.1 + 0.9 \cdot \frac{W_i(t) - W_{min}(t)}{W_{max}(t) - W_{min}(t)}. \quad (7)$$

$W_{max}(t)$ and $W_{min}(t)$ denote the maximal and minimal wear at the current time step t . The normalized wear for the tire with the lowest wear is set to 0.1, the tire with the highest wear is set to 1.0.

3) *Motor Temperature*: A maximal temperature for the motors and power electronics in the experimental vehicle is defined. To reduce wear, the optimizer tries to avoid critical temperature states by keeping the temperature of the components well below this threshold. Alternatively, an optimal target temperature could have been defined. A first-order lag element serves as simple model of the temperature development of the motor when demanding a certain torque. More complex models could be used for higher precision of temperature prediction as, e. g., presented by [15]. For basic prediction, a first-order lag element has proven to deliver sufficient precision and reduces computational load. The predicted temperatures of all components are normalized:

$$n_T(t) = \frac{T(t + \Delta t) - T_a}{T_{max} - T_a} \quad (8)$$

T_a and T_{max} denote the ambient temperature and the maximal acceptable temperature of a motor, respectively.

4) *Battery State of Charge*: The SOC of a battery is monitored based on the current pack voltage. This is a strong simplification but experimental results have shown that the SOC of the batteries in the experimental vehicle is approximated sufficiently, and the basic operation of the presented algorithm can be demonstrated. More complex battery models to estimate the SOC depending on the used type of battery are investigated by several research groups, e. g., by Sen et al. [4]. The normalized state of charge n_B of the battery at the current point in time t is calculated as:

$$n_B(t) = \frac{V_{max} - V_{meas}(t)}{V_{max} - V_{min}}. \quad (9)$$

Thereby, V_{max} and V_{min} denote the maximal and minimal allowed pack voltage, $V_{meas}(t)$ the measured voltage. Thus, the normalized value can change between 0 (fully charged battery) and 1 (empty battery).

C. Dynamic Weighting

To improve the optimization results and integrate expert knowledge into the system, the presented normalized optimization criteria are weighted before they are provided to the optimization algorithm. Due to the normalization, these weights define the absolute importance of each individual criterion also across different types of optimization criteria.

For weighting of the criteria, a unified weighting curve according to the formula:

$$weight(\eta) = 1 + \frac{1}{e^{-(C_1 \cdot \eta - C_2)} + C_3} \quad (10)$$

is introduced. The parameters C_1 , C_2 and C_3 are set individually for each of the optimization criteria. The input value η resembles the normalized absolute tire wear, the percentage of maximal acceptable temperature, or the percentage of minimal acceptable pack voltage rated from 0 to 1.

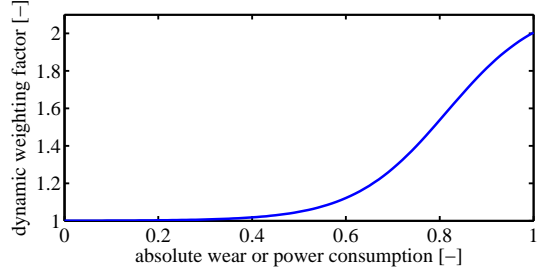


Fig. 5. Curve of dynamic weighting factor of optimization criteria

Fig. 5 illustrates the weighting curve for the parameters $C_1 = 10$, $C_2 = 8$ and $C_3 = 0.86$. The weighting curve is designed to increase the weight of an optimization criterion if it gets closer to the absolute wear or energy limit of the component. The flattening of the curve towards the maximum serves to limit the weight of one criterion even if for some reason one component is used up to a critical level or beyond. The range of values is chosen to be 1 to 2 and not 0 to 1 in order to ensure that all optimization criteria can be weighted with a predefined static weighting factor at any time. The static weighting factor multiplies the return value of Equ. 10. All components apart from torque deviation are weighted equally (static weight = 1). Torque deviation is weighted inversely to the temperature, battery SOC and tire wear criteria and scaled by a minimal factor of 20 to stress the importance of this optimization goal:

$$weight_{torque} = 40 - 20 \cdot \max(\text{other weights}) \quad (11)$$

Due to the inverse weighting, torque reduction is facilitated if other components reach critical states.

V. EXPERIMENTAL RESULTS

A 1:5 scale model and simulations based on a non-linear double track model form the basis for evaluation of the optimization approach. The scale model is a functional model of a full scale prototype that is built up in parallel to this research project. With the scale vehicle the real-time performance of the approach is demonstrated. The experimental vehicle and the vehicle dynamics simulation are configured as four wheel drive vehicle with one electric motor per axle and independent steering of the front wheels.

A. Comparison: Evolutionary MOMBES vs. SQP Algorithm

Fig. 6 shows the tire wear balancing results for the SQP and MOMBES optimization algorithm for a 73.5s test run with arbitrary course. Both optimization systems are triggered every 0.15s of simulation time.

MOMBES balances tire wear throughout the drive. From the pareto frontier provided by MOMBES, the solution with

the lowest overall tire wear parameter tw is chosen. tw is calculated as sum of all tire wear values and the deviation of each individual wear value from the average wear of all tires. SQP cannot achieve the same quality of results (total wear and balancing) but approximates the optimal solution. The execution time of SQP is significantly lower than the one of MOMBES. The evolutionary algorithm requires more than 9 hours to perform all required calculations on a 2.16 Ghz Intel Dual Core platform. The SQP algorithm requires less than one minute for the same virtual test drive. A real-time execution of the SQP algorithm on the onboard Intel Atom 1.6 GHz processor is possible.

Identification of global optima by the SQP algorithm can be improved by the multi-start strategy. If the deviations in tire wear surpass a given threshold, four SQP optimization routines with different starting points are started in parallel for one time step. The starting points are generated such that a set of reasonable torque and steering distributions is resembled. Afterwards, the solution with minimal wear is chosen. The positive effect of the multi-start phase can be seen in Fig. 6. At about 22s a multi-start cycle facilitates shift to a better, potentially global, minimum.

B. Tire Wear Benchmark

To demonstrate real-time capabilities and performance of the presented approach, tire wear generated during a test drive using an optimized steering geometry is compared to the tire wear generated by an ackermann steering geometry. Therefore, the model vehicle accelerates to $2\frac{m}{s}$ (corresponding to approx. $10\frac{m}{s}$ in full scale) on a straight segment and then turns into a constant left curve with a steering angle of 15 degree. For this driving scenario, ackermann steering resembles a good benchmark as this steering geometry is designed to generate little tire wear at low speeds. Fig. 7 shows the tire wear for the front wheels and the rear axle calculated according to the formulas introduced in Sec. IV-B2 during a real test drive. The sum of left and right steering angle for the optimized geometry is constrained to the sum of steering angles for the ackermann steering geometry. This

generates comparable handling of the experimental vehicle during the test runs. The tire wear values of the rear wheels are not regarded separately as the optimization algorithm has no possibility to balance the wear between left and right wheel in the current vehicle configuration. Instead, the mean value for left and right wheel is provided to the optimization system and illustrated in Fig. 7.

The optimizer balances the wear between front and rear axle and left and right wheels of the front axle. The wear of the wheel with highest load is reduced significantly by shifting drive power partially to the rear axle and increasing side slip at the curve-inner front wheel to take over an increasing part of the lateral forces. Due to nonlinear increase of tire wear with increasing load, the total wear for optimized driving is reduced slightly to 97.5% of the wear generated by the ackermann steering geometry. Still, the simplified tire wear estimation formula used in this paper lacks precision for detailed benchmarks on absolute wear.

C. Battery Charge Levels

Fig. 8 shows the reaction of the optimization system to dropping voltage in the drive batteries during a simulated test run. Thereby, a speed controller tries to keep a constant vehicle speed on a straight segment. A battery pack voltage of 10V is set as critical cut-off voltage and the voltage levels of the two batteries are initialized to different levels. While the voltage is well above the critical level, the sum of the torque distribution factors set for front and rear axle is close to 200%. As soon as one battery nears the critical level, the optimizer tries to balance the battery levels by changing the torque distribution. At the end of the drive, the vehicle is forced to a stop as both battery levels are critical. The "virtual driver" detects the upcoming stop at about 24 s of simulation time as a significant increase in accelerator pedal command is required to keep the commanded speed.

D. Motor Temperatures

Motor temperature is regarded by the optimizer to avoid overheating. The maximal temperature for the motors is set to

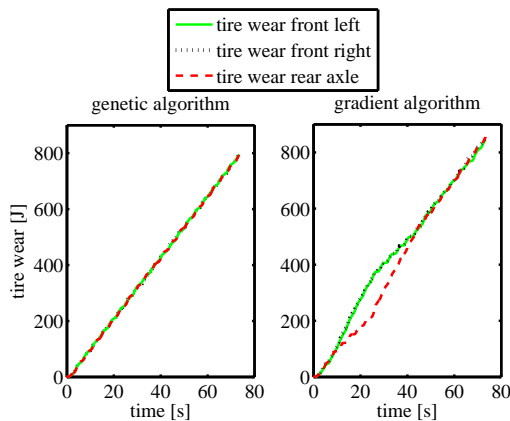


Fig. 6. Tire wear balancing for evolutionary and gradient based optimization

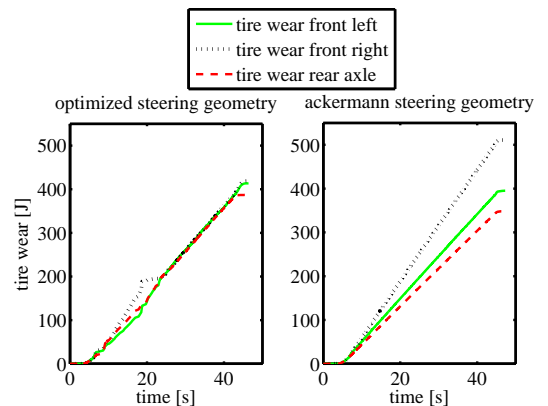


Fig. 7. Tire wear for driving a constant left curve with optimized steering geometry and ackermann steering geometry

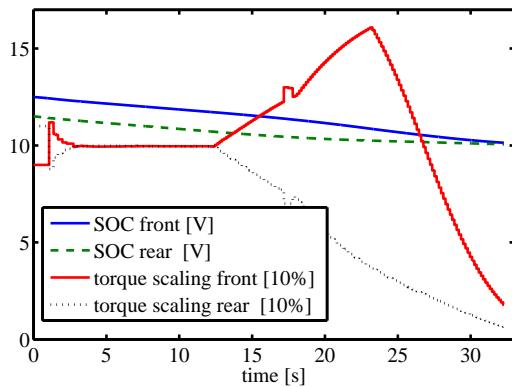


Fig. 8. Battery pack voltage and torque distribution factors

70 degree celsius. A straight acceleration serves as test scenario. Fig. 9 shows the torque commanded by the driver and the torque request sent to each of the motors. During main acceleration, torque commands are limited due to overheating of the motors. As soon as both motors have cooled down sufficiently (after about 120 s), the optimization algorithm increasingly starts to balance wear deviations between front and rear axle introduced by the acceleration scenario. Thus non-critical differences in motor temperature result.

E. Influence of Execution Frequency

Fig. 10 illustrates the standard deviation of all tire wear values for a course with several curves and straight sections for different execution frequencies of the optimization system. The standard deviation increases almost linearly with decreasing execution frequency and thus indicates reduced quality of the optimization results. Obviously, the tire wear criterion imposes high demands on execution frequency to allow proper optimization. Still, the chosen architecture decouples optimization task and vehicle control well.

VI. CONCLUSION

This paper proposes an approach to optimize wear and energy distribution in vehicles and limit overloads of com-

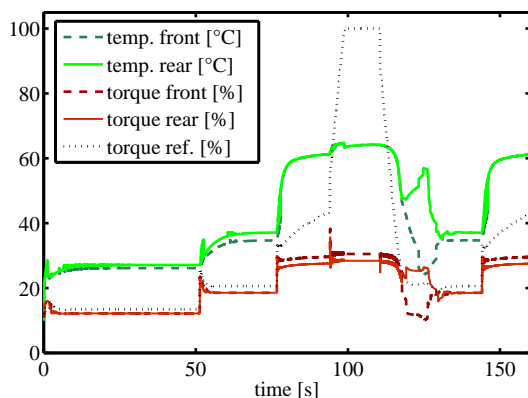


Fig. 9. Temperature curves during simulation

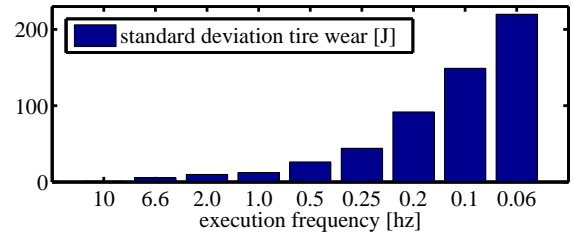


Fig. 10. Standard deviation of tire wear values depending on the execution frequency of the optimization algorithm (SQP)

ponents based on classical optimization algorithms. The approach does not replace protection measures for individual components, but can improve the performance of the overall system. As a result, the system helps to increase life time of the overall vehicle. The demonstration scenario showed that the approach can be applied to highly real-time critical applications in vehicles. Thereby, the system performance is scalable depending on the available computational resources. Future work will focus on further evaluation of the proposed approach in a full scale experimental vehicle with independent four wheel steering and drive.

REFERENCES

- [1] Yu, Hai; Liang, Wei; Kuang, Ming; Mcgee, Ryan: "Vehicle Handling Assistant Control System via Independent Rear Axle Torque Biasing", *2009 American Control Conference*, 2009, pp. 695-700.
- [2] Ringdorfer, M.; Horn, M.: "Development of a wheel slip actuator controller for electric vehicles using energy recuperation and hydraulic brake control", *2011 IEEE International Conference on Control Applications (CCA)*, 2011, pp. 313-318.
- [3] Mitchell, W. C.; Staniforth, A.; Scott, I.: Analysis of Ackermann Steering Geometry, *SAE Technical Papers Series 2006-01-3638*, 2006.
- [4] Sen, C.; Kar, N. C.: "Battery Pack Modeling for the Analysis of Battery Management System of a Hybrid Electric Vehicle", *Vehicle Power and Propulsion Conference, IEEE VPPC '09*, 2009, pp.207-212.
- [5] Chen, C.; Jin, J.; He, L.: "A New Battery Management System for Li-ion Battery Packs", *IEEE Asia Pacific Conference on Circuits and Systems, APCCAS 2008*, 2008, pp.1312-1315.
- [6] Robert Bosch GmbH (editor): *Automotive Electrics - Automotive Electronics*, 5th Edition, Wiley-Blackwell, Oxford, 2008.
- [7] BMW AG: Start-Stop Technology, www.bmw.com (Feb. 21st 2012).
- [8] Alcaraz, J.; Maroto, C.: "A Robust Genetic Algorithm for Resource Allocation in Project Scheduling", *Annals of Operations Research 102*, 2001, pp. 83-109.
- [9] Zhang, H.; Xu, H.; Peng, W.: "A Genetic Algorithm for Solving RCPSP", *International Symposium on Computer Science and Computational Technology*, 2008, pp. 246-249.
- [10] Meyer, D. (editor): *Model-based Multi-objective Optimization with Neural Networks and Evolution Strategies*, [Dissertation], Frankfurt/Oder, Technischen Universität Ilmenau, 2003.
- [11] Powell, M.J.D.: "A fast algorithm for nonlinearly constrained optimization calculations", *Lecture Notes in Mathematics*, Volume 630, 1978, pp. 144-157.
- [12] Schittkowski, K.: "NLPQL: A fortran subroutine solving constrained nonlinear programming problems", *Annals of Operations Research 5*, 1985, pp. 485-500.
- [13] Huang, H.; Yu, G.; Gang, Z.: Wear-Optimal Design: A Tire Wear Model and Sensitivity Analysis, *Computer, Mechatronics, Control and Electronic Engineering (CMCE)*, vol.6, 2010, pp. 414-417.
- [14] Kiencke, U.; Nielsen, L.: *Automotive Control Systems*, Springer-Verlag, Berlin-Heidelberg, 2005.
- [15] Schröder, D. (editor) (in German): *Elektrische Antriebe - Grundlagen*, Springer-Verlag, Berlin Heidelberg, 4.Auflage, 2009.